
Exploring Misclassifications of Robust Neural Networks to Enhance Adversarial Attacks

Leo Schwinn, René Raab, An Nguyen, Dario Zanca, Bjoern Eskofier

Department Artificial Intelligence in Biomedical Engineering, Univ. of Erlangen-Nürnberg, Germany
{leo.schwinn, rene.raab, an.nguyen, dario.zanca, bjoern.eskofier}@fau.de

Abstract

Progress in making neural networks more robust against adversarial attacks is mostly marginal, despite the great efforts of the research community. Moreover, the robustness evaluation is often imprecise, making it difficult to identify promising approaches. We analyze the classification decisions of 19 different state-of-the-art neural networks trained to be robust against adversarial attacks. Our findings suggest that current untargeted adversarial attacks induce misclassification towards only a limited amount of different classes. Additionally, we observe that both over- and under-confidence in model predictions result in an inaccurate assessment of model robustness. Based on these observations, we propose a novel loss function for adversarial attacks that consistently improves attack success rate compared to prior loss functions for 19 out of 19 analyzed models.

1 Introduction

Deep Neural Networks (DNNs) can be easily fooled into making wrong predictions by seemingly negligible perturbations to their input data, called adversarial examples. Szegedy et al. [26] first demonstrated the existence of adversarial examples for neural networks in the image domain. Since then, adversarial examples have been identified in various other domains such as speech recognition [21] and natural language processing [18]. This prevalence of adversarial examples has severe security implications for real-world applications. As a result, the robustness of neural networks to adversarial examples has become a central research topic of deep learning in recent years.

Several defense strategies have been proposed to make DNNs more robust [3, 6, 10, 17]. However, most of them have later been shown to be ineffective against stronger attacks [13, 20] and overall progress has been slow [4]. As robustness improvements are mostly marginal, a reliable evaluation of new defense strategies is critical to identify methods that actually improve robustness. Therefore, the community has established helpful guidelines to reliably evaluate new defenses [1, 27, 28]. Nevertheless, the worst-case robustness of DNNs is still reduced repetitively by even stronger attacks and a precise evaluation remains a challenging problem [4]. Moreover, prior work focuses on evaluating the robustness of individual DNNs without bringing them into the context of other models.

In this work, we explore the classification decisions of 19 recently published DNNs. Hereby, we restrict our analysis to DNNs which have been trained to be robust against adversarial attacks with a variety of different methods. Our analysis can be summarized by two main findings: First, we observe that untargeted adversarial attacks cause misclassification towards only a limited amount of different classes in the dataset. Second, we identify three model properties that make it difficult to accurately assess model robustness – namely, model over- and under-confidence, large output logits, and irregular input gradient geometry. We leverage these observations to design a new loss function that improves the success rate of adversarial attacks compared to current state-of-the-art loss functions. More specifically, we encourage attack diversity in untargeted attacks by injecting noise to the model output. Additionally, we introduce scale invariance to the loss function by normalizing the output

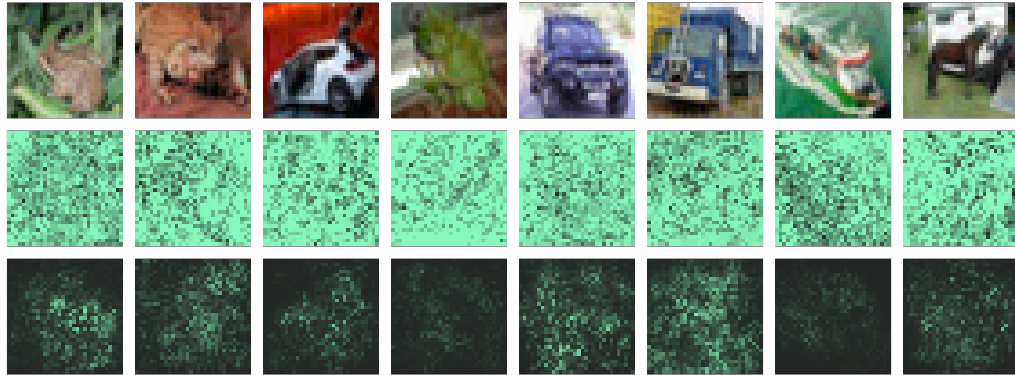


Figure 1: Difference of adversarial perturbations created by Cross-Entropy (CE)-based attacks and Jitter-based attacks. Original images are shown in the first row, CE-based perturbations in the second row, and Jitter-based perturbations in the last row.

logits to a fixed value range. Thereby, we circumvent the gradient obfuscation problem generated by models with low-confidence predictions or irregularly large output logits [2, 4]. Moreover, we propose a simple yet effective mechanism that minimizes the magnitude of perturbations, as shown in Figure 1, without compromising the success rate of an attack. This leads to the definition of an objective function for adversarial attacks, which we will refer to as *Jitter*. We empirically evaluate our loss function on an extensive benchmark consisting of 19 different models proposed in the literature. We show that Jitter-based attacks consistently improve the success rate compared to prior loss functions in all 19 models by up to 13.8 percentage points. Additionally, Jitter-based attacks generate perturbations with a 2.85 times smaller norm on average. Lastly, we analyze the effect of Jitter on the classification decisions to explain its effectiveness.

2 Notation

Let $f_\theta : [0, 1]^d \rightarrow \mathbb{R}^C$ be a DNN classifier parameterized by $\theta \in \Theta$ with $f_\theta : x \mapsto z$. Here x is a d -dimensional input image, z is the respective output vector (logits) of the DNN, and C denotes the number of classes. The ground truth class label of a given image is described by $y \in \{1, \dots, C\}$ while the predicted class label $\hat{y} \in \{1, \dots, C\}$ is given by $\text{argmax}(z)$.

Adversarial examples $x_{adv} = x + \gamma$ aim to change the input data of DNNs such that the classification decision of the network is altered, but the class label remains the same for human perception. Additionally, x_{adv} is restricted to remain within the data domain, i.e. $x_{adv} \in [0, 1]^d$. A common way to enforce semantic similarity to the original sample is to restrict the magnitude ϵ of the adversarial perturbation γ by a ℓ_p -norm bound, such that $\|\gamma\|_p \leq \epsilon$. We refer to the set of valid adversarial examples that fulfill these constraints as S . As prior work mainly focuses on $p = \infty$ and thus most models are available for this threat model, we focus on $p = \infty$ in this work as well. Furthermore, we restrict our analysis to untargeted white-box adversarial attacks.

3 Related work

One of the most often used adversarial attacks, Projected Gradient Descent (PGD), was proposed by Madry et al. [17]. PGD is an iterative gradient-based attack, in which multiple smaller gradient updates are used to find the adversarial perturbation:

$$x_{adv}^{t+1} = \Pi_S(x_{adv}^t + \alpha \cdot \text{sign}(\nabla_x \mathcal{L}(f_\theta(x_{adv}^t), y))) \quad (1)$$

where $0 < \alpha \leq \epsilon$ and x_{adv}^t describes the adversarial example at iteration t . The loss of the attack is given by $\mathcal{L}(f_\theta(x_{adv}^t), y)$. $\Pi_S(x)$ is a projection operator that keeps γ^t within the set of valid perturbations S and sign is the component-wise signum operator. The starting point of the attack x_{adv}^0 is randomly chosen in the ϵ -norm ball. More variants of iterative gradient-based attacks have been proposed that are more effective than vanilla PGD [16, 24, 28]. Recently, Croce and Hein

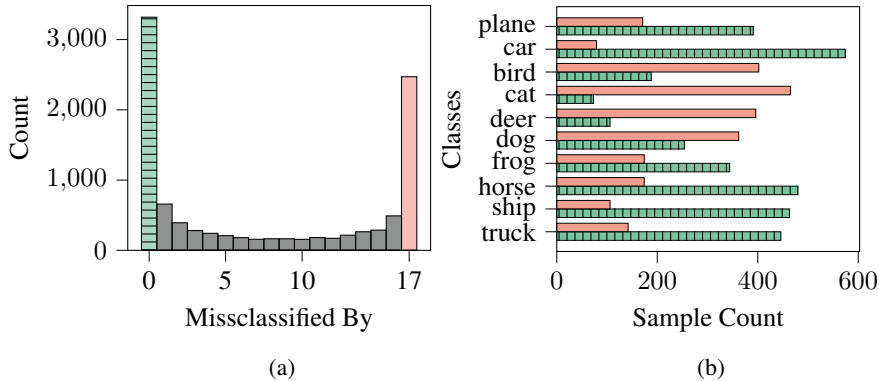


Figure 2: Analysis of misclassification decisions for 17 different models. Subfigure (a) shows by how many models each attacked input is misclassified. Robust images that are never misclassified are shown in the leftmost column (green, dashed) and non-robust images that are always misclassified are shown in the rightmost column (red). Subfigure (b) displays the difference between the class distributions between robust and non-robust images. Both statistics are calculated on the test set of CIFAR10.

[4] proposed the Auto-PGD (APGD) attack. In contrast to previous PGD versions, APGD requires considerably less hyperparameter tuning and was shown to be more effective than other PGD-based attacks against a variety of models [4]. Nevertheless, one important component of all gradient-based attacks is their optimization objective. The most often used objective is the Cross-Entropy (CE) loss. Carlini and Wagner [2] observe that CE-based attacks fail against models with large logits. They propose the Carlini & Wagner (CW) loss function $-z_y + \max_{i \neq y}(z_i)$ which does not make use of the softmax function and thereby reduces the scaling problem. Nevertheless, Croce and Hein [4] observe that the scale dependence of the CW loss can still lead to severe failure cases against models with exceptionally large logits. They address this issue with the scale- and shift-invariant Difference of Logit Ratio (DLR) loss and show its effectiveness on an extensive benchmark.

4 Robust misclassifications

In this section we explore the classification decisions of 19 different models in the presence of adversarial attacks. We restrict our analysis to models trained on the CIFAR10 dataset.¹ We choose the recently proposed Auto-PGD (APGD) with the Difference of Logit Ratio (DLR) loss as an attack to perturb the images, as it is one of the most efficient and reliable gradient-based attacks [4]. These choices and specific hyperparameters are described in more detail in Section 6.

4.1 Distribution of misclassifications

Recent studies mainly focus on common evaluation metrics to assess the robustness of DNNs. This includes the worst-case robustness of a classifier [4] and the magnitude of the perturbation norm necessary to fool the classifier for individual inputs [2]. Here, we provide insights into the classification decisions and numerical properties of a large and diverse set of models from the literature. We focus on models that are trained to be robust to adversarial attacks. Furthermore, all models are attacked individually to find the respective worst-case robustness.

Figure 2a shows how the 17 most robust models misclassify inputs attacked by APGD. We left out the models by Jin and Rinard [13] and Mustafa et al. [19] from this analysis, as they show negligible robustness against strong adversarial attacks. Out of the 10,000 test samples of the CIFAR10 dataset, 3319 are correctly classified by all 17 models, while 2471 samples are consistently misclassified by all models. This is shown by the leftmost (green, dashed) and rightmost (red) bar of the histogram plot. Inspired by prior work [12], we will refer to images in the first group that are never misclassified as *robust images* and images in the second group that are always misclassified as *non-robust images*. The gray bars in between show the remaining 4210 samples misclassified by at least one model but

¹The labels "airplane" and "automobile" have been changed to "plane" and "car", respectively

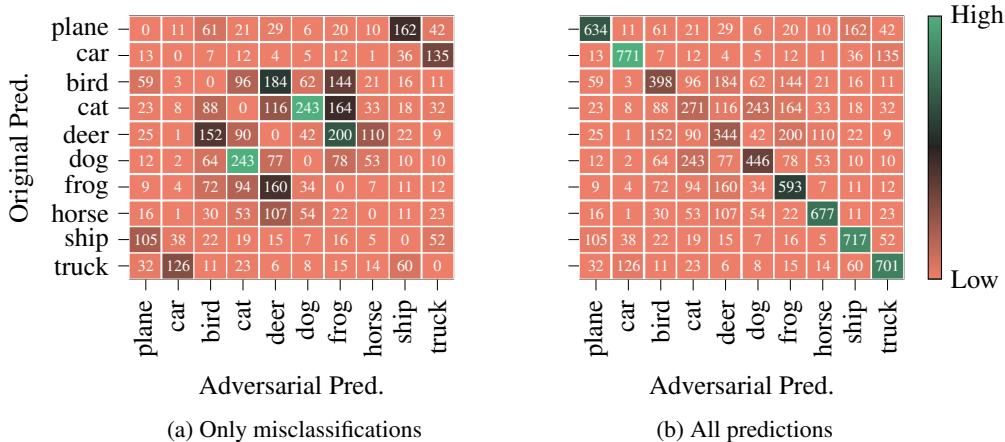


Figure 3: Averaged confusion matrices of all models for adversarially perturbed inputs. Subfigure (a) shows the confusion matrix for only successful attacks while subfigure (b) shows all predictions. Both matrices are calculated on the test set of CIFAR10.

not by all models. Figure 2b summarizes the class distribution of robust and non-robust images. There is a considerable difference in frequency for most classes between the two groups. Images from the classes "plane", "car", "horse", "ship", and "truck" are often classified correctly while "bird", "cat", "deer" and "dog" are mostly misclassified.

We additionally explored the average of the confusion matrices of all models for adversarially perturbed images. Note that the CIFAR10 dataset is balanced and contains an equal amount of samples for all classes. Figure 3a shows the confusion matrix of only the misclassifications, while Figure 3b shows the whole confusion matrix. It can be seen that the matrix in Figure 3a contains only a few large values, which is in line with the previous observation that some classes are easier to perturb than others. Furthermore, the matrix is largely symmetric. Classes are mainly confused amongst pairs. This includes semantically meaningful pairs such as "cats" and "dogs" or "car" and "truck", but it also includes other pairs that generally share similar image backgrounds such as "plane" and "ship", "deer" and "frog", and "deer" and "bird". Examples of robust images and non-robust images are included in the appendix.

4.2 Model properties

Here, we first analyze the distribution of the output logits z and subsequently inspect the input gradient geometry of the different models [23]. We then relate these properties to the difficulty of the robustness evaluation. Models that display irregular properties are highlighted with gray shading and text in Figure 4.

Prior work observed that simply scaling the output of a DNN will lead to vanishing gradients when the softmax function is used in the last layer of the network [4, 9]. This phenomenon occurs due to finite arithmetic and thus limited precision, where the CE loss is quantized to 0 and the model effectively obfuscates the gradient from the attack. The CE loss is given by:

$$\text{CE}(z, y) = -\log(\text{softmax}(z)_y) \text{ where } \text{softmax}(z)_y = \frac{e^{z_y}}{\sum_{j=1}^C e^{z_j}}. \quad (2)$$

Figure 4a summarizes the logit distributions of all models. The model proposed by Mustafa et al. [19] shows large logits, which lead to precision issues as described above. Furthermore, the models by Mustafa et al. [19] and Ding et al. [6] exhibit a considerably higher average confidence (0.948) than all other models (0.666 excluding models with exceptionally low confidence [13, 20]). In contrast, the models by Jin and Rinard [13] and Pang et al. [20] reveal a different phenomenon where the logits are close to zero and show a substantially lower standard deviation than the other models. Consequently, the logits are generally mapped to a limited value range by the softmax function, where all values are similar. Thus, the loss may only change slightly between different attack iterations,

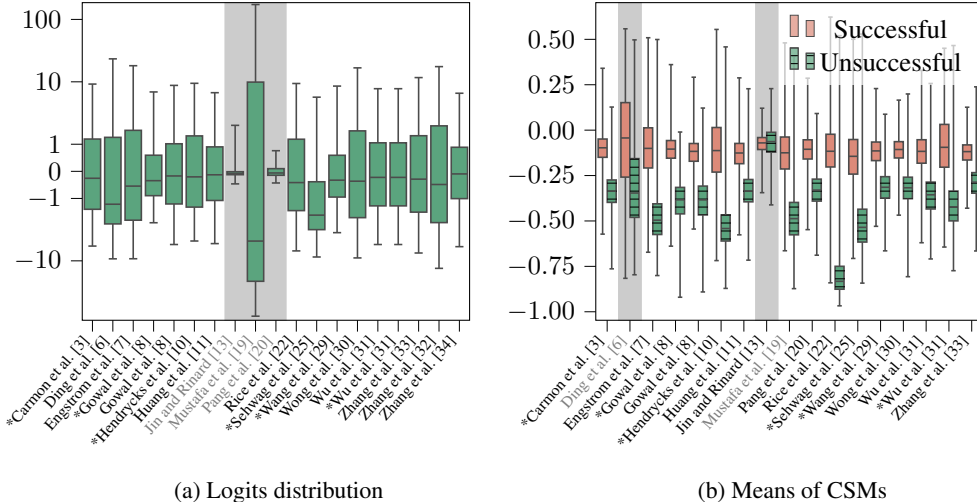


Figure 4: (a) Box plots of the logits distribution of clean images from the CIFAR10 test set for all models analyzed in this paper. (b) Box plots of the means of the CSMs calculated with the GGA method for both robust (green, dashed) and non-robust (red) images [23]. The models highlighted by gray shading and text show considerably lower robustness against strong attacks compared to standard PGD [6, 13, 19, 20]. Models that use additional data during training are marked with a *.

which subsequently decreases the attack performance. This is also reflected in low confidence for the two models, where the most confident prediction has a probability of < 0.51 while it is ≈ 1 for all other models. The confidence distribution for all models is given in the appendix.

We further analyzed if robust and non-robust images exhibit different properties with the Geometric Gradient Analysis (GGA) method proposed by Schwinn et al. [23]. GGA is used to identify untrustworthy predictions (e.g., adversarial examples) by analyzing the geometry of the saliency maps for a given sample through the computation of Cosine Similarity Matrices (CSMs). In this experiment, we analyzed the clean version of the images. Figure 4b shows a considerable difference between the distribution of the mean values of the CSMs for non-robust images (red) and robust images (green, dashed). This indicates a different response of the DNNs for non-robust and robust images even if the images are not perturbed. Furthermore, the two models proposed by Ding et al. [6] and Pang et al. [20] (gray shaded area) display a different behavior for the CSM mean values. For those models, the mean values between robust and non-robust images differ only slightly and the box plots overlap while they are substantially different for the other models.

All 4 models identified in the above analysis show high robustness against CE-based attacks. However, for these 4 models, the difference between a standard robustness evaluation with CE-based PGD and stronger attacks is larger than 7% and considerably less accurate than for the other 15 models [5].

5 Enhancing adversarial attacks

In the previous section, we explored the misclassification of robust DNNs under adversarial attacks. The experiments showed a general consistency between the different models. Specifically, we discovered that common attacks mostly focus on a limited amount of different classes to attack in the untargeted setting. Additionally, we observed that the scale and distribution of the output logits are linked to the success rate of adversarial attacks. Based on these observations, we now design a novel loss function for adversarial attacks to make them more effective. We first describe the two main components of this loss function. Subsequently, we elaborate how we can minimize the norm of the final adversarial perturbation without compromising the attack’s success rate. This is important as adversarial attacks should not change the label for human perception, which is linked to the perturbation magnitude.

Scale invariance: Previous work already demonstrated that high output logits can lead to gradient obfuscation and weaken adversarial attacks [2, 4]. We additionally observe that a small value range

Table 1: Ablation results for the individual Jitter components for the model proposed by Jin and Rinard [13]

Attack	Accuracy	Improvement
APGD _{CE}	52.34	N/A
APGD _{CE} & Scaled	18.29	+34.05
APGD _{Scaled} & L2	18.13	+0.16
APGD _{Scaled} & L2 & Jitter	7.54	+10.59

of the logits can also lead to attack failure. We propose to scale the softmax function by the following rule:

$$\hat{z} = \text{softmax} \left(\alpha \cdot \frac{z}{\|z\|_\infty} \right) \quad (3)$$

where α is an easy-to-tune scalar value that controls the lowest and largest possible output values of the softmax function.

Encouraging diverse attack targets: Figure 3 demonstrates that untargeted adversarial attacks mainly induce misclassifications for a limited amount of classes. We argue that this behavior limits the effectiveness of adversarial attacks. This notion is supported by prior work that showed that performing targeted attacks against every possible class is usually more effective than applying a single untargeted attack [4, 15]. However, these so-called multi-targeted attacks are computationally expensive and do not scale to datasets with a high number of output classes. We propose to exchange the CE loss function with the Euclidean distance between the rescaled softmax output \hat{z} and the one-hot encoded ground truth vector Y . The Euclidean distance increases fastest by maximizing the magnitude of any of the output logits where $z_i \neq z_y$, which simultaneously minimizes the distance between Y and z_y . Combining the euclidean loss function and the scaling described in (3) the loss function can be described by the following equation.

$$\mathcal{L}_2 = \|\hat{z} - Y\|_2. \quad (4)$$

To encourage the attack to explore different gradient directions we additionally perturb the logits after each forward pass with Gaussian noise, where the noise magnitude is controlled by the hyperparameter σ . The resulting loss function is given by:

$$\mathcal{L}_{Noise} = \|\hat{z} + \mathcal{N}(0, \sigma) - Y\|_2. \quad (5)$$

Note that this method does not improve the performance when using the CE loss in our experiments. This is expected as the CE loss is only dependent on the output of the ground truth class and adding noise to the other output values has no impact.

Minimizing the norm of the perturbation Finally, we aim to encourage the attack to find small perturbations. As long as no successful perturbation is found, we apply the loss function presented in (5). Once the adversarial attack is successful we additionally consider the norm of the adversarial perturbation. Furthermore, we only override the current perturbation if the newly found perturbation also leads to a successful attack. This procedure can never decrease the success rate of the attack and effectively minimizes the norm of the adversarial perturbation in our experiments. Moreover, the norm (or other distance measure) can be freely chosen according to the respective problem (e.g., ℓ_1 , ℓ_2 , ℓ_∞) as long as it is differentiable. The final loss function can be described as follows:

$$\mathcal{L}_{Jitter} = \begin{cases} \frac{\|\hat{z} - Y + \mathcal{N}(0, \sigma)\|_2}{\|\gamma\|_p} & \text{if } x_{adv} \text{ is misclassified} \\ \|\hat{z} - Y + \mathcal{N}(0, \sigma)\|_2 & \text{if } x_{adv} \text{ is not misclassified yet} \end{cases} \quad (6)$$

Table 2: Accuracy of the evaluated models when attacked with APGD using different loss functions. The difference between the best and second-best loss function is given in the right-most column. The most successful attack is highlighted in bold while the second most successful attack is underlined and models that use additional data are marked with a *.

Model	CE	CW	DLR	Jitter	Diff.
Mustafa et al. [19]	19.12	0.10	<u>0.05</u>	0.02	-0.03
Jin and Rinard [13]	52.33	47.78	<u>21.33</u>	7.54	-13.8
Wong et al. [30]	<u>45.83</u>	45.95	47.05	44.49	-1.34
Zhang et al. [32]	46.12	47.15	47.71	46.01	-0.11
Ding et al. [6]	<u>50.13</u>	51.07	51.29	47.85	-2.29
Engstrom et al. [7]	<u>51.77</u>	52.27	53.09	51.08	-0.69
Zhang et al. [33]	54.80	<u>53.53</u>	53.64	53.05	-0.48
Huang et al. [11]	55.86	<u>53.94</u>	54.41	53.33	-0.60
Zhang et al. [34]	56.84	<u>54.49</u>	54.77	53.98	-0.51
Rice et al. [22]	56.89	<u>55.36</u>	56.00	54.36	-1.00
Pang et al. [20]	61.62	<u>55.44</u>	56.28	54.48	-0.96
*Hendrycks et al. [10]	57.15	<u>56.44</u>	57.23	55.94	-0.50
Wu et al. [31]	58.80	<u>56.76</u>	56.82	56.45	-0.31
Gowal et al. [8]	59.50	<u>57.82</u>	<u>57.60</u>	57.09	-0.51
*Wang et al. [29]	61.82	<u>58.23</u>	58.95	57.58	-0.64
*Schwag et al. [25]	59.61	<u>58.30</u>	58.45	57.66	-0.65
*Carmon et al. [3]	61.73	<u>60.61</u>	60.88	60.08	-0.52
*Wu et al. [31]	63.32	<u>60.62</u>	60.67	60.44	-0.18
*Gowal et al. [8]	65.69	<u>63.75</u>	63.92	63.31	-0.45

The effect of the different components is exemplified in Table 1 for the model proposed in [13]. Every component decreases the accuracy of the model and therefore increases the success rate of the attack. Note that the norm minimization does not affect the performance and is excluded.

6 Experiments

We conducted a series of experiments to evaluate the effectiveness of the proposed Jitter loss function. Furthermore, we inspect the perturbations generated with the Jitter loss function to explain its effectiveness compared to other state-of-the-art loss functions.

Data and models All experiments were performed on the CIFAR10 dataset [14]. We chose CIFAR10 as it is one of the most often used datasets to evaluate adversarial robustness. We gathered 19 models from the literature for the attack evaluation. All models are either taken from the RobustBench library [5] or from the GitHub repositories of the authors directly [13, 19]. We only consider models which are trained to be robust against ℓ_∞ -norm attacks. The resulting benchmark contains a diverse set of models which are trained with different methods.

Threat model We compare the performance of different loss functions for the Auto-PGD (APGD) attack [4], which consistently beats other iterative gradient-based attacks. Moreover, APGD has no hyperparameters such as step size and thus enables a less biased comparison between different loss functions. We compare Jitter to three different loss functions. First of all, the CE loss which is the standard loss function for training supervised DNNs and is the most often used loss function for gradient-based adversarial attacks. The CW loss proposed by Carlini and Wagner [2] that shows considerably better results compared to CE when the model shows high output logits. The DLR loss proposed in [4] that was shown get more stable results compared to the CE and CW loss. All attacks are untargeted ℓ_∞ -norm attacks with $\epsilon = 8/255$ and use 100 attack iterations.

Jitter Hyperparameter Compared to CE and DLR, Jitter introduces two additional hyperparameters. The first hyperparameter α rescales the softmax input and directly controls the possible minimum and maximum value of the output logits and the average magnitude of the gradient. Note that values for α close to or greater than ≈ 83 will result in an overflow of 32-bit float values in the softmax function and thereby to numerical issues (see Section 4.2). Thus, we can focus on $0 < \alpha \ll 83$. In a preliminary experiment, we explored different values for α between 2 and 20 and observed a

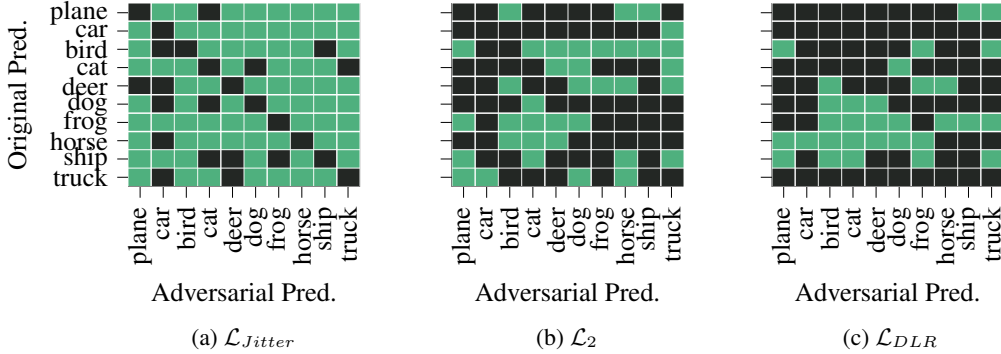


Figure 5: Illustration of the diversity of targeted classes for \mathcal{L}_{Jitter} -based, \mathcal{L}_2 -based, and \mathcal{L}_{DLR} -based attacks. Subfigure (a), (b), and (c) show binarized confusion matrices for the different attacks, where more green squares indicate a higher attack diversity.

stable performance over all values. We chose $\alpha = 10$ for all remaining experiments. The second hyperparameter σ controls the amount of noise added to the rescaled softmax output \hat{z} . We tuned σ for every model individually on a batch of 100 samples by testing values for $\sigma \in \{0, 0.05, 0.1, 0.15, 0.2\}$. Note that tuning σ on a small batch for each model introduces only a negligible overhead ($\approx 1\%$ additional runtime).

7 Results and discussion

7.1 Attack performance

Table 2 compares the performance of the different loss functions on the CIFAR10 dataset. The best result for every model is highlighted in bold. The difference between the best and second-best attack is shown in the rightmost column. The proposed Jitter loss achieves superior performance compared to all other loss functions for all models. For the model proposed in [13], Jitter achieves a 13.8% higher success rate than the second best loss function and a 44.8% higher success rate than the commonly used CE loss. Moreover, the Jitter loss is the only loss function that is consistently better than the other loss functions. In contrast, the other three loss functions differ in performance for every model. The CE loss is better than CW and DLR in 4 out of 19 cases, the CW loss is better than CE and DLR in 12 out of 19 cases, and the DLR loss is better than CE and CW in 3 out of 19 cases. To evaluate the performance of Jitter with a higher computational budget we compared DLR and Jitter using 1000 model evaluations (5 restarts and 200 iterations). While the success rate increased up to 6.51% for Jitter, the high budget version of DLR performed worse than 100 iteration Jitter in all cases. An extensive overview is given in the appendix.

7.2 Induced Misclassifications

We designed Jitter to increase the diversity of target classes for untargeted adversarial attacks. Figure 5 displays binarized confusion matrices of the model proposed in [6] for the APGD attack. We compare the proposed \mathcal{L}_{Jitter} loss to \mathcal{L}_{DLR} for which we observed the relative sparsity of the confusion matrices in Figure 3a. Additionally, we investigate the \mathcal{L}_2 loss function given in (4) to evaluate the effect of adding Gaussian noise the output logits. We chose the model proposed by Ding et al. [6], as both \mathcal{L}_{DLR} and \mathcal{L}_2 show a considerable performance gap ($> 3\%$) compared to \mathcal{L}_{Jitter} for this model. In the subfigures 5a, 5b, and 5c green squares denote that an attack changed the classification decision to the respective class at least once. \mathcal{L}_{Jitter} -based attacks show a considerably higher amount of different target classes compared to the other two attacks. This indicates that adding noise to the logits increases the diversity of an attack. Moreover, \mathcal{L}_{DLR} -based attacks were not able to successfully attack the classes car and truck which explains the performance difference to \mathcal{L}_{Jitter} .

Furthermore, we analyzed the final adversarial perturbations found with Jitter-based attacks and CE-based attacks for the same model [6]. Figure 6 shows the CW loss [2] on the y -axis along the direction of an adversarial perturbation on the x -axis for both loss functions. We choose the CW

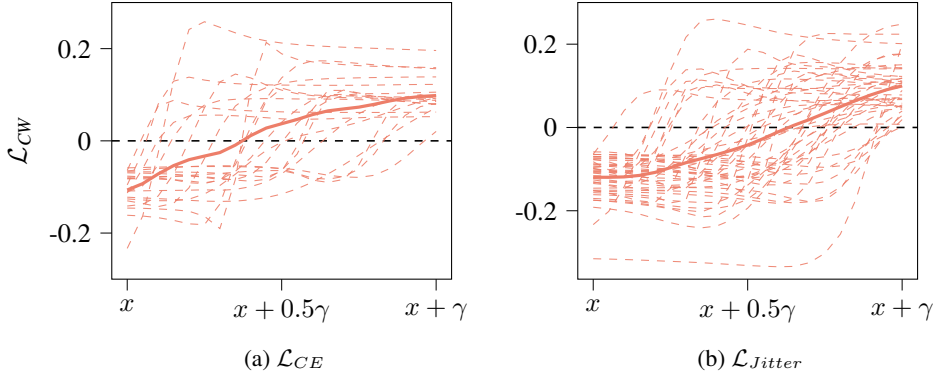


Figure 6: Analysis of the final adversarial perturbation found for \mathcal{L}_{CE} -based and \mathcal{L}_{Jitter} -based attacks. The CW loss [2] is shown on the y-axis along the direction of an adversarial attack. Here x describes a clean image and $x + \gamma$ the adversarial example.

loss as it can directly be related to the classification decision of a classifier (inputs with $\mathcal{L}_{CW} > 0$ are misclassified). The subfigures show the individual loss values for 50 randomly drawn samples of the test set as dashed lines. The mean value over the whole test set for each group is shown by a solid line. CE-based attacks generally find adversarial directions which directly increase the CW loss. On the other hand, Jitter-based attacks mainly find adversarial directions which do not directly increase the CW loss, which can be seen by the constant mean near the clean input x . Moreover, the mean CW loss value of Jitter-based attacks exceeds the threshold of misclassification noticeably later than CE-based attacks (Jitter:0.63, CE:0.42). CE-based attacks always follow the direction of the steepest ascent. In contrast, Jitter-based attacks are forced to do more exploration due to the additional noise. This enables Jitter-based attacks to find perturbation directions that are sub-optimal in the beginning but lead to a misclassification at the final adversarial perturbation.

7.3 Attack norm and structure

In a final experiment, we examined the average perturbation norm of the different attack configurations for all 19 models. We choose to minimize the ℓ_2 norm with Jitter, as differences in the ℓ_2 norm are easier to interpret than for the ℓ_∞ norm (e.g. the attack focusing on specific regions). The average ℓ_2 perturbation norm over all samples for the different loss functions is: CE:0.52, CW:0.56, DLR:0.55, and Jitter:0.19. A more extensive overview is given in the appendix. We also inspect the structure of the perturbations. Figure 1 displays the perturbation for CE- and Jitter-based attacks for several images. To plot the perturbations, we calculate the absolute sum over every color channel and show the magnitude as a color gradient, where no change is denoted by black color. CE-based attacks generally attack every pixel in an image. In comparison, Jitter-based attacks mainly focus on the salient regions of an image. We argue that focusing on the most distinct image regions enables Jitter-based attacks to create successful low-norm adversarial attacks.

8 Conclusion and outlook

In this paper, we analyze the classification decisions of a diverse set of models that are trained to be adversarially robust. We utilize insights of our analysis to create a novel loss function which we name Jitter that increases the success rate of adversarial attacks. Specifically, we enforce scale invariance of the loss function and encourage a diverse set of target classes for the attack by adding Gaussian noise to the output logits. The proposed method shows superior attack success rates for 19 out of 19 models compared to three other popular loss functions in the literature. Moreover, the average perturbation norm of Jitter-based attacks is considerably lower compared to prior methods, which is achieved without compromising the success rate of the attack. Future work will explore automatic tuning of the noise injection to the output logits for every individual sample during an attack.

References

- [1] Anish Athalye, Nicholas Carlini, and David A. Wagner. Obfuscated gradients give a false sense of security: Circumventing defenses to adversarial examples. In *Proceedings of the 35th International Conference on Machine Learning, ICML*, volume 80 of *Proceedings of Machine Learning Research*, pages 274–283. PMLR, 2018.
- [2] Nicholas Carlini and David A. Wagner. Towards evaluating the robustness of neural networks. In *2017 IEEE Symposium on Security and Privacy, SP*, pages 39–57. IEEE Computer Society, 2017.
- [3] Yair Carmon, Aditi Raghunathan, Ludwig Schmidt, John C. Duchi, and Percy Liang. Unlabeled data improves adversarial robustness. In *Advances in Neural Information Processing Systems 32, NeurIPS*, pages 11190–11201, 2019.
- [4] Francesco Croce and Matthias Hein. Reliable evaluation of adversarial robustness with an ensemble of diverse parameter-free attacks. In *Proceedings of the 37th International Conference on Machine Learning, ICML*, volume 119, pages 2206–2216. PMLR, 2020.
- [5] Francesco Croce, Maksym Andriushchenko, Vikash Sehwal, Nicolas Flammarion, Mung Chiang, Prateek Mittal, and Matthias Hein. Robustbench: a standardized adversarial robustness benchmark. *CoRR*, abs/2010.09670, 2020.
- [6] Gavin Weiguang Ding, Yash Sharma, Kry Yik Chau Lui, and Ruitong Huang. MMA training: Direct input space margin maximization through adversarial training. In *8th International Conference on Learning Representations, ICLR*, 2020.
- [7] Logan Engstrom, Andrew Ilyas, Hadi Salman, Shibani Santurkar, and Dimitris Tsipras. Robustness (python library), 2019. URL <https://github.com/MadryLab/robustness>. [Accessed May 25th, 2021].
- [8] Sven Gowal, Chongli Qin, Jonathan Uesato, Timothy A. Mann, and Pushmeet Kohli. Uncovering the limits of adversarial training against norm-bounded adversarial examples. *CoRR*, abs/2010.03593, 2020.
- [9] Kartik Gupta and Thalaiyasingam Ajanthan. Improved gradient based adversarial attacks for quantized networks. *CoRR*, abs/2003.13511, 2020.
- [10] Dan Hendrycks, Kimin Lee, and Mantas Mazeika. Using pre-training can improve model robustness and uncertainty. In *Proceedings of the 36th International Conference on Machine Learning, ICML*, volume 97 of *Proceedings of Machine Learning Research*, pages 2712–2721. PMLR, 2019.
- [11] Lang Huang, Chao Zhang, and Hongyang Zhang. Self-adaptive training: beyond empirical risk minimization. In *Advances in Neural Information Processing Systems 33, NeurIPS*, 2020.
- [12] Andrew Ilyas, Shibani Santurkar, Dimitris Tsipras, Logan Engstrom, Brandon Tran, and Aleksander Madry. Adversarial examples are not bugs, they are features. In *Advances in Neural Information Processing Systems 32, NeurIPS*, pages 125–136, 2019.
- [13] Charles Jin and Martin Rinard. Manifold regularization for adversarial robustness. *CoRR*, abs/2003.04286, 2020.
- [14] Alex Krizhevsky. Learning multiple layers of features from tiny images. Technical report, 2009.
- [15] Hyun Kwon, Yongchul Kim, Ki-Woong Park, Hyunsoo Yoon, and Daeseon Choi. Multi-targeted adversarial example in evasion attack on deep neural network. *IEEE Access*, 6:46084–46096, 2018.
- [16] Jiadong Lin, Chuanbiao Song, Kun He, Liwei Wang, and John E. Hopcroft. Nesterov accelerated gradient and scale invariance for adversarial attacks. In *8th International Conference on Learning Representations, ICLR*, 2020.

- [17] Aleksander Madry, Aleksandar Makelov, Ludwig Schmidt, Dimitris Tsipras, and Adrian Vladu. Towards deep learning models resistant to adversarial attacks. In *6th International Conference on Learning Representations, ICLR*, 2018.
- [18] John X. Morris, Eli Lifland, Jin Yong Yoo, Jake Grigsby, Di Jin, and Yanjun Qi. Textattack: A framework for adversarial attacks, data augmentation, and adversarial training in NLP. In *Proceedings of the 2020 Conference on Empirical Methods in Natural Language Processing: System Demonstrations, EMNLP - Demos*, pages 119–126. Association for Computational Linguistics, 2020.
- [19] Aamir Mustafa, Salman H. Khan, Munawar Hayat, Roland Goecke, Jianbing Shen, and Ling Shao. Adversarial defense by restricting the hidden space of deep neural networks. In *IEEE/CVF International Conference on Computer Vision, ICCV*, pages 3384–3393. IEEE, 2019.
- [20] Tianyu Pang, Xiao Yang, Yinpeng Dong, Taufik Xu, Jun Zhu, and Hang Su. Boosting adversarial training with hypersphere embedding. In *Advances in Neural Information Processing Systems 33, NeurIPS*, 2020.
- [21] Yao Qin, Nicholas Carlini, Garrison W. Cottrell, Ian J. Goodfellow, and Colin Raffel. Imperceptible, robust, and targeted adversarial examples for automatic speech recognition. In *Proceedings of the 36th International Conference on Machine Learning, ICML*, volume 97 of *Proceedings of Machine Learning Research*, pages 5231–5240. PMLR, 2019.
- [22] Leslie Rice, Eric Wong, and J. Zico Kolter. Overfitting in adversarially robust deep learning. In *Proceedings of the 37th International Conference on Machine Learning, ICML*, volume 119 of *Proceedings of Machine Learning Research*, pages 8093–8104. PMLR, 2020.
- [23] Leo Schwinn, An Nguyen, René Raab, Leon Bungert, Daniel Tenbrinck, Dario Zanca, Martin Burger, and Bjoern Eskofier. Identifying untrustworthy predictions in neural networks by geometric gradient analysis. *CoRR*, abs/2102.12196, 2021.
- [24] Leo Schwinn, An Nguyen, René Raab, Dario Zanca, Bjoern Eskofier, Daniel Tenbrinck, and Martin Burger. Dynamically sampled nonlocal gradients for stronger adversarial attacks. *CoRR*, abs/2011.02707, 2021.
- [25] Vikash Sehwal, Shiqi Wang, Prateek Mittal, and Suman Jana. HYDRA: pruning adversarially robust neural networks. In *Advances in Neural Information Processing Systems 33, NeurIPS*, 2020.
- [26] Christian Szegedy, Wojciech Zaremba, Ilya Sutskever, Joan Bruna, Dumitru Erhan, Ian J. Goodfellow, and Rob Fergus. Intriguing properties of neural networks. In *2nd International Conference on Learning Representations, ICLR*, 2014.
- [27] Florian Tramèr, Nicholas Carlini, Wieland Brendel, and Aleksander Madry. On adaptive attacks to adversarial example defenses. *CoRR*, abs/2002.08347, 2020.
- [28] Jonathan Uesato, Brendan O’Donoghue, Pushmeet Kohli, and Aäron van den Oord. Adversarial risk and the dangers of evaluating against weak attacks. In *Proceedings of the 35th International Conference on Machine Learning, ICML*, pages 5025–5034, 2018.
- [29] Yisen Wang, Difan Zou, Jinfeng Yi, James Bailey, Xingjun Ma, and Quanquan Gu. Improving adversarial robustness requires revisiting misclassified examples. In *8th International Conference on Learning Representations, ICLR*, 2020.
- [30] Eric Wong, Leslie Rice, and J. Zico Kolter. Fast is better than free: Revisiting adversarial training. In *8th International Conference on Learning Representations, ICLR*, 2020.
- [31] Dongxian Wu, Shu-Tao Xia, and Yisen Wang. Adversarial weight perturbation helps robust generalization. In *Advances in Neural Information Processing Systems 33, NeurIPS*, 2020.
- [32] Dinghuai Zhang, Tianyuan Zhang, Yiping Lu, Zhanxing Zhu, and Bin Dong. You only propagate once: Accelerating adversarial training via maximal principle. In *Advances in Neural Information Processing Systems 32, NeurIPS*, pages 227–238, 2019.

- [33] Hongyang Zhang, Yaodong Yu, Jiantao Jiao, Eric P. Xing, Laurent El Ghaoui, and Michael I. Jordan. Theoretically principled trade-off between robustness and accuracy. In *Proceedings of the 36th International Conference on Machine Learning, ICML*, volume 97 of *Proceedings of Machine Learning Research*, pages 7472–7482. PMLR, 2019.
- [34] Jingfeng Zhang, Xilie Xu, Bo Han, Gang Niu, Lizhen Cui, Masashi Sugiyama, and Mohan S. Kankanhalli. Attacks which do not kill training make adversarial learning stronger. In *Proceedings of the 37th International Conference on Machine Learning, ICML*, volume 119 of *Proceedings of Machine Learning Research*, pages 11278–11287. PMLR, 2020.

A Appendix

A.1 Robust and non-robust images

In Figure 7 we display examples of robust and non-robust images. Specifically, we show images that are correctly classified by all models under normal conditions but are misclassified when attacked. Moreover, we focus on images where all models predict the same wrong target class. These images contain semantically interesting examples:

- A ship in the air that is classified as a plane.
- A golf cart that is labeled as a car but classified as a truck.
- An ambulance that is labeled as a car but classified as a truck.

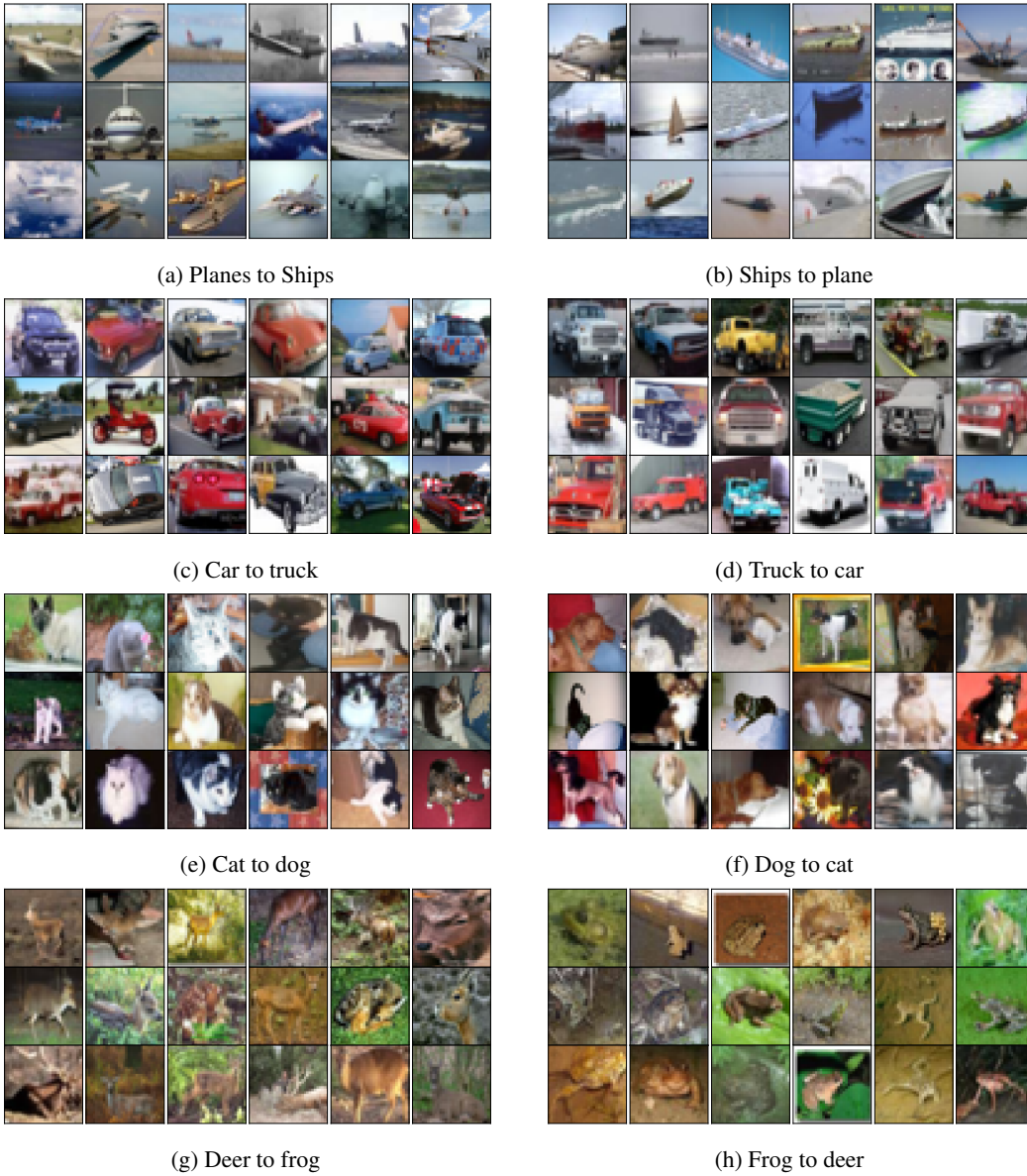


Figure 7: Images that are correctly classified by all models under normal conditions but misclassified by all models under attack (DLR-based APGD). Examples of images that are misclassified as the same target class (e.g., cat images that are always misclassified as dogs) are shown.

A.2 Model confidence distribution

We observed that models that show under- or over-confident predictions on average are more difficult to attack with standard attacks. The confidence distribution for all models is summarized in Figure 8. Models that are either under- or over-confident are highlighted by gray shading and text.

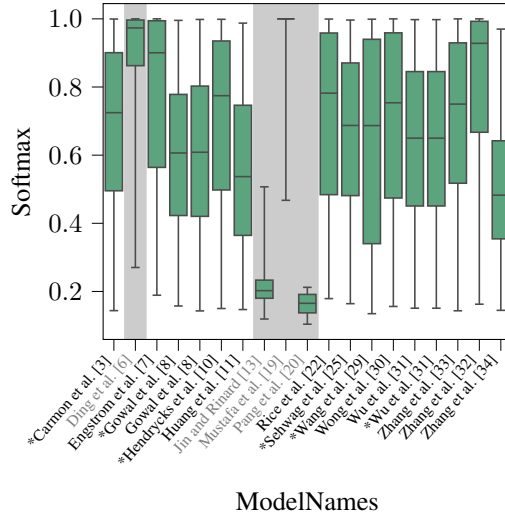


Figure 8: Confidence distribution of all models. Only the highest softmax output for every prediction is considered.

A.3 Attack norm

The distribution of the ℓ_2 norm perturbation magnitude is displayed in Figure 9. Jitter-based attacks exhibit perturbations with smaller norms compared to attacks with the other three loss functions in all cases.

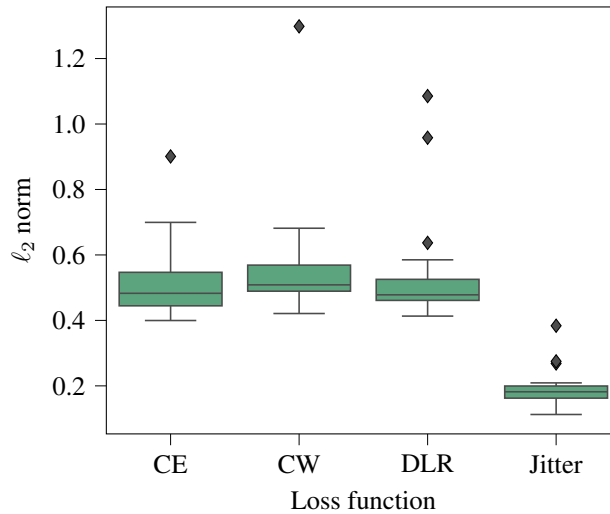


Figure 9: Analysis of the ℓ_2 norm perturbation magnitude between the different loss functions. The box plots show the quartiles of the data while the whiskers extend to 95% of the value range.

A.4 Attack performance for a higher computational budget

The performance of DLR- and Jitter-based attacks for more model evaluations is shown in Table 3. Attacks with a "strong" suffix use 200 iterations and 5 restarts, while the other attacks use 100

iterations without additional restarts. Low-budget Jitter-based attacks achieve a higher success rate than both normal and strong DLR-based attacks in all cases. Overall more model evaluations do only marginally improve the performance for DLR-based attacks except for the model proposed by Jin and Rinard [13], where the success rate increases by 8.9 percentage points. For Jitter-based attacks more model evaluations improve the performance considerably for the models proposed by Jin and Rinard [13] and Ding et al. [6] and slightly for the models proposed by Wong et al. [30], Rice et al. [22], and Hendrycks et al. [10].

Table 3: Accuracy [%] of the evaluated models when attacked with APGD using either the DLR or Jitter loss function. Attacks with a "strong" suffix use 200 iterations and 5 restarts, while the other attacks use 100 iterations without additional restarts.

Models	DLR	Jitter	DLR Strong	Jitter Strong	Diff.
Mustafa et al. [19]	0.05	0.02	0.03	0.00	0.02
Jin and Rinard [13]	21.33	7.54	12.43	1.03	6.51
Wong et al. [30]	47.05	44.49	46.69	43.45	1.04
Ding et al. [6]	51.29	47.85	50.19	43.62	4.23
Zhang et al. [32]	47.71	46.01	47.31	45.79	0.22
Engstrom et al. [7]	53.09	51.08	52.59	50.83	0.24
Zhang et al. [33]	53.64	53.05	53.42	52.88	0.17
Huang et al. [11]	54.41	53.33	54.24	53.25	0.09
Zhang et al. [34]	54.77	53.98	54.54	53.64	0.34
Rice et al. [22]	56.00	54.36	55.70	53.66	0.70
Pang et al. [20]	56.28	54.48	55.97	54.10	0.38
Hendrycks et al. [10]	57.23	55.94	56.98	55.10	0.84
Wu et al. [31]	56.82	56.45	56.69	56.10	0.35
Gowal et al. [8]	57.60	57.09	57.44	57.08	0.01
Wang et al. [29]	58.95	57.58	58.55	57.28	0.31
Sehwag et al. [25]	58.45	57.66	58.23	57.50	0.15
Carmon et al. [3]	60.88	60.08	60.62	59.90	0.19
Wu et al. [31]	60.67	60.44	60.56	60.19	0.25
Gowal et al. [8]	63.92	63.31	63.74	62.73	0.57

A.5 Jitter Code

The following algorithm shows a PyTorch-like implementation of Jitter.

Algorithm 1 Code for the Jitter loss in a PyTorch-like fashion

```
# X: input data, X_adv: adversarial input data, B: batch size
# z: logits, y: labels, Y: one-hot encoded labels
# alpha: value range, sigma: noise magnitude, norm: norm to minimize

##### logit scaling #####
z_scaled = z / norm(z.view(B, -1), p=float("inf"), dim=1, keepdim=True)
z_scaled = softmax(z_scaled * alpha, dim=1)
z_noisy = z_scaled + randn_like(z_scaled) * sigma
##### l2 loss #####
l2 = norm((z_noisy - Y).view(B, -1), p=2, dim=1)
##### perturbation magnitude #####
non_adversarial_mask = z.argmax(1) != y
magnitude = norm((X - X_adv).view(B, -1), p=norm, dim=1)
masked_magnitude = ones_like(l2)
masked_magnitude[non_adversarial_mask] = magnitude[non_adversarial_mask]
##### final loss #####
loss = l2 / masked_magnitude
return loss
```
